LAWRENCE
LIVERMORE
NATIONAL
LABORATORY

UCRL-JRNL-230670

Development of a Cell-Based Fluorescence Resonance Energy Transfer Reporter for Bacillus anthracis Lethal Factor Protease

R. H. Kimura, E. R. Steenblock, J. A. Camarero

May 2, 2007

Analytical Biochemistry

Development of a Cell-Based Fluorescence Resonance Energy Transfer Reporter for *Bacillus anthracis* Lethal Factor Protease

Richard Kimura, Erin R. Steenblock and Julio A. Camarero*

Biosciences and Biotechnology Division, Livermore National Laboratory, University of California, 7000 East Avenue, L-231, Livermore, CA 94550, USA.

Phone: (925) 422-6807, E-mail: camarero1@llnl.gov.

Running Title: Cell-based reporter for Anthrax Lethal Factor Protease

Abstract

We report the construction of a cell-based fluorescent reporter for anthrax lethal factor (LF) protease activity using the principle of fluorescence resonance energy transfer (FRET). This was accomplished by engineering an *Escherichia coli* cell line to express a genetically encoded FRET reporter and LF protease. Both proteins were encoded in two different expression plasmids under the control of different tightly controlled inducible promoters. The FRET-based reporter was designed to contain a LF recognition sequence flanked by the FRET pair formed by CyPet and YPet fluorescent proteins. The length of the linker between both fluorescent proteins was optimized using a flexible peptide linker containing several Gly-Gly-Ser repeats. Our results indicate that this FRET-based LF reporter was readily expressed in *E. coli* cells showing high levels of FRET *in vivo* in the absence of LF. The FRET signal, however, decreased 5 times after inducing LF expression in the same cell. These results suggest that this cell-based LF FRET reporter may be used to screen genetically encoded libraries *in vivo* against LF.

Keywords: Anthrax, FRET-based reporter, cell biosensing, metalloprotease, *in vivo* screening.

Introduction

The exposure of U.S. postal workers to *Bacillus anthracis,* the pathogen causing anthrax, in 2001 revealed a gap in the nation's overall preparedness against bioterrorism.

B. anthracis infections are difficult to treat because flu-like symptoms appear only after the bacteria have multiplied inside the human host and started to produce the corresponding bacterial toxin that eventually causes death. If classical antibiotics are applied at this stage, the infection can be still lethal because of the accumulation of the corresponding bacterial toxin. A pharmacological agent that directly targets the toxin might thus prove to have a valuable synergy with more traditional antibacterial treatments.

The high pathogenicity of anthrax is mostly due to rapid bacterial growth combined with the secretion of three powerful exotoxin components: edema factor (EF), lethal factor (LF), and protective antigen (PA). EF is a calcium and calmodulin-dependent adenylate cyclase (AC) that converts cellular ATP into cyclic AMP (cAMP) [1]. LF is a Zn^{2+}-dependent metalloprotease [2] that cleaves and inactivates mitogen-activated protein kinase kinases (MAPKKs) [3]. PA binds to a cell surface anthrax toxin receptor (ATR/TEM-8 or CMG-2) [4; 5; 6] where it is activated by proteolytic cleavage by furin-like proteases [7]. This step enables the formation of an heptameric pore [8] that allows cellular entry of LF and EF. Once inside the cell, LF and EF cause extensive cellular damage to the host cell defense system. Although the complete mechanism of pathogenesis is not yet fully understood, the disruption of key signaling pathways mediated by MAPKKs seems to lead first to the lysis of macrophages [9; 10], impairment of dendritic cells and later to the death of the host [11]. The pivotal role of LF in the virulence of the toxin suggests that inhibitors of this enzyme may provide protection against cytotoxicity.

The first step in the design of potential inhibitors is the development of a rapid, sensitive, and simple assay for testing a large number of compounds, usually referred as libraries [12; 13; 14]. Classical methods for LF assays, such as HPLC [15] and SDS-PAGE [16; 17], are impractical for high-throughput screening of compound libraries, either of chemical or biological origin. The development of new fluorescence-based substrates, however, has opened the door for high-throughput screening of LF inhibitors [18; 19; 20]. Optimized synthetic peptides containing various types of fluorophores have been reported for fast, sensitive, and robust assays suited for high-throughput screening [13; 21].

In recent years, the introduction of green fluorescent protein (GFP) to fluorescence resonance emission transfer (FRET)-based activity assays has introduced a new avenue to study proteases and their inhibitors inside living cells [22; 23]. The recent design of fluorescent proteins optimized for FRET [24] has enabled for the first time the use of new high-throughput screening applications using sensitive fluorescence-activated cell sorting (FACS) [24; 25].

The combination of FACS with FRET-based genetically encoded proteolytic reporters allows the possibility for *in vivo* screening of protease inhibitors using chemically generated [12; 13] or biologically encoded libraries [14]. The later possibility suggests an even more intriguing scenario in which single cells can be used as individual microfactories for the biosynthesis and screening of particular inhibitors in a single process within the same cellular cytoplasm [26]. This strategy also has the advantage in that the screening process takes place in a complex molecular environment, which provides the ideal background for the selection of highly specific inhibitors.

Recent developments in the fields of molecular biology and protein engineering have now made possible the *in vivo* biosynthesis of cyclic peptide–based combinatorial libraries [27;

28; 29; 30; 31; 32] that can be screened *in vivo* against LF. Interestingly, several natural products, including defensin peptides [33; 34] and aminoglycosides [35], have been recently shown to inactivate LF factor.

Key to the idea of using genetically encoded cell libraries for the *in vivo* screening of potential inhibitors against LF using FACS is the development of a robust cell-based fluorescent assay for LF. In the present work, we report an *Escherichia coli* cell line that has been engineered to express both LF protease and a FRET-based LF substrate under the control of two orthogonal and inducible bacterial promoters. The FRET-based LF substrate was designed to contain a consensus LF recognition sequence [36] flanked by a FRET pair of optimized fluorescent proteins, a cyan fluorescent protein (CyPet) and yellow fluorescent protein (YPet) [24]. Several tandem CyPet–YPet fusion proteins with different linkers were generated and evaluated *in vitro* for maximum substrate accessibility, while maintaining high FRET efficiency. The fluorescent LF reporter was readily expressed in *E. coli* showing high levels of FRET *in vivo* in the absence of LF. Conversely, the FRET signal was significantly reduced when LF and its FRET-based substrate were sequentially expressed in the same cell line. Our results demonstrate that this cell-based FRET reporter for LF can be used to screen *in vivo* for LF inhibitors.

Materials and methods

General materials and methods. Analytical HPLC was performed on an HP1100 series instrument with 220-nm and 280-nm detection using a Vydac C18 column (5 μm, 4.6 x 150 mm) at a flow rate of 1 mL/min. Semipreparative HPLC was performed on a Waters Delta Prep system fitted with a Waters 2487 Ultraviolet-Visible (UV-vis) detector using a Vydac C18 column (15–20 μm, 10 x 250 mm) at a flow rate of 5 mL/min. All runs used linear gradients of

0.1% aqueous trifluoroacetic acid (TFA, solvent A) vs. 0.1% TFA, 90% acetonitrile in H_2O (solvent B). UV-vis spectroscopy was carried out on an Agilent 8453 diode array spectrophotometer, and fluorescence analysis was performed on a Spex FluoroLog-3 spectrofluorometer (Jobin Yvon). Electrospray mass spectrometry (ES-MS) analysis was routinely applied to all protein constructs. ES-MS was performed on an MDS Sciex API-150EX single quadrupole electrospray mass spectrometer. Calculated masses were obtained by using ProMac v1.5.3. Protein samples were analyzed by SDS-PAGE on 4–20% Tris-Glycine Gels (Invitrogen). SDS-PAGE gels were stained with Pierce Gelcode Blue or Silversnap II stain kits, photographed/digitized using a Kodak EDAS 290, and quantified using NIH Image-J software (http://rsb.info.nih.gov/ij/). DNA sequencing was performed at Davis Sequencing facility (Davis, CA) using an ABI 3730 DNA sequencer. The sequence data were analyzed with Lasergene v5.5.2 (DNAStar). All chemicals were obtained from Sigma-Aldrich unless otherwise indicated.

Solid-phase peptide synthesis of the LF consensus peptide (H-RRKKVYPYPMEGTIA-OH). Peptide synthesis was manually performed using the HBTU activation protocol for Fmoc solid-phase peptide synthesis [37] on a 4-Fmoc-Rink amide resin (Novabiochem). Coupling yields were monitored by the quantitative ninhydrin determination of residual free amine [38]. Protected N^{α}-Fmoc amino acids were purchased from Novabiochem. Side-chain protection was employed as previously described for the Fmoc protocol. Methionine was introduced as unprotected Fmoc-Met-OH.

*Construction of CyPet–YPet fusion protein reporters (**1** to **6**).* The CyPet–YPet parent bacterial expression construct containing both optimized CyPet and YPet [24] was engineered as follows. First, DNA encoding CyPet was obtained by PCR amplification using the pCyPet-His plasmid [24] as a template. The DNA amplicon was then inserted into the *Nhe*I and *Bam*HI sites

of the T7 expression vector pET28a(+) (Novagen) to give plasmid pET28a-CyPet. In a second step, DNA encoding YPet was produced by PCR amplification using the pYPet-His plasmid [24] as a template. This DNA was inserted in frame into the *Hind*III and *Xho*I sites of pET28a-CyPet to give plasmid pET28a-CyPet-YPet. The forward and reverse primers employed for the PCR amplification of the DNA encoding for CyPet are 5'-GGC CAG GAG TGC TAG CAT GTC TAA AGG TG-3' and 5'-GGT GGT GGT GGG ATC CTT TGT ACA ATT CAT CC-3', respectively. The forward and reverse primers employed for PCR amplification of the DNA encoding for YPet are 5'-CAC TAA GGC CAG GAA AGC TTC GAT GTC TAA AGG-3' and 5'-CCT TAG TGG TGG TGC TCG AGT TAT TTG TAC AAT-3', respectively. In all the cases, the resulting PCR amplicons and plasmids were digested with their respective restriction endonucleases (NEB) and purified by gel using the QIAquick Gel Extraction Kit (Qiagen) prior to ligation with T4 DNA ligase (NEB). The DNA encoding the LF substrate consensus sequence [36] was cloned into the plasmid pET28a-CyPet-YPet using the *Bam*HI and *Hind*III sites. Different inserts encoding the LF substrate flanked by various repeats of the flexible tripeptide GGS were prepared (Figure 1). Constructs **1**, **2**, **3**, **4,** and **5** encoded 0, 1, 2, 4, and 6 pairs of the tripeptide GGS, respectively, and were prepared as follows. 5'-Phosphorylated top (p5) and bottom (p3) strand oligonucleotides were synthesized by IDT DNA (Coralville, IA) (Table 1). Complementary strands were annealed in 20 mM sodium phosphate, 0.3 M NaCl buffer at pH 7.4 and the resulting double-stranded DNA (dsDNA) was purified using QIAquick PCR Purification Kit (Qiagen). In plasmids encoding constructs **4** and **5**, the dsDNA inserts were constructed by first ligating the dsDNA resulting from annealing oligonucleotides p5a-p3a and p5b-p3b (see Table 1). The resulting dsDNA was 5'-phosphorylated with T4 PNK (NEB). This strategy was employed due to the decreased yield and purity associated with synthetic

oligonucleotides larger than 100 bases. All the dsDNA inserts were introduced in frame into the *Bam*HI and *Xho*III sites of pET28a-CyPet-Ypet to give plasmids pET28a-1 to pET28a-5.

Reporter protein construct **6** is similar to construct **5** but it was cloned into the expression vector pBAD/Myc-HisA (Invitrogen) using the *Sac*I and *Kpn*I restriction sites to give plasmid pBAD-6. Forward and reverse primers containing *Sac*I and *Kpn*I, respectively, were used to amplify by PCR the DNA encoding construct **5** using pET28a-5 as a template. The resulting amplicon was inserted into the *Sac*I and *Kpn*I sites of the expression vector pBAD/Myc-HisA. The forward and reverse primer sequences used in the PCR amplification are 5'-ATA TAT GAG CTC TAG CAT GTC TAA AGG TGA AGA-3' and 5'-AAT ATA GGT ACC TTG TAC AAT TCA TTC ATA CCC-3', respectively.

All plasmids were first transformed into competent *E. coli* DH5α cells (Invitrogen) and plated on Luria broth (LB)-agar containing either kanamycin (34 mg/L) for the pET28a-derived vectors or ampicillin (100 mg/L) for the pBAD-derived vector. Positive colonies were grown in 5 mL of LB containing the appropriate antibiotic at 37°C overnight and the corresponding plasmid purified using a miniprep kit (Qiagen). Plasmids were either screened by PCR using the same cloning primers or by digestion using the same restriction endonucleases used for cloning. Positive plasmids were sequenced and screened for bacterial expression.

*Expression and purification of CyPet–YPet fusion protein reporters (**1** to **5**). E. coli* Rosetta 2(DE3) cells (Novagen) were transformed with plasmids pET28a-1 to pET28a-5. Expression was carried out in 1 L of LB medium containing ampicillin (100 mg/L) and chloramphenicol (34 mg/L) at 20°C overnight. Briefly, 5 mL of an overnight starter culture derived from a single clone was used to inoculate 1 L of LB media. Cells were grown to an OD at 600 nm of ≈ 0.5 at 37°C, and expression was induced by the addition of isopropyl-β-D-

thiogalactosidase (IPTG) to a final concentration of 0.25 mM at 20°C overnight. The cells were harvested by centrifugation, resuspended in 30 mL of lysis buffer (0.1 mM PMSF, 25 mM sodium phosphate, 150 mM NaCl buffer at pH 8.0 containing 5% glycerol) and lysed by sonication. The lysate was clarified by centrifugation at 15,000 rpm in a Sorval SS-34 rotor for 30 minutes. The clarified supernatant was incubated with 1 mL of Ni-NTA agarose beads (Qiagen) previously equilibrated with column buffer (25 mM sodium phosphate, 150 mM NaCl buffer at pH 8.0) at 4°C for 1 hour with gentle rocking. The Ni-NTA agarose beads were washed sequentially with column buffer containing 10 mM imidazole (100 mL) followed by column buffer containing 20 mM imidazole (100 mL). The fusion protein was eluted with 2 mL of column buffer containing 100 mM EDTA. Proteins were characterized as the desired product by ES-MS (see Figure 1). Quantification of the CyPet–YPet fusion proteins was carried out spectrophotometrically using an extinction coefficient per chain at 517 nm of 104,000 $M^{-1}cm^{-1}$ [22; 24]. Approximately 10 mg of FRET reporter protein were purified per 1 L of culture grown as indicated above.

Construction of LF protease expression vector (pRSF-LF). The DNA encoding LF protease from *B. anthracis* strain Sterne was isolated by PCR using the pTXB1-LF plasmid [20] as a template. The forward (5'-TAA GGA TCC GGC GGG CGG TCA TGG TGA-3') and reverse (5'-GCA TCT CCC GTG ATG CAG GAA-3') primers contained a *Bam*HI and *Not*I restriction site, respectively. The resulting amplicon was purified using Qiagen's PCR purification kit, digested and ligated into *Bam*HI- and *Not*I-treated plasmid pRSFDuet-1 (Novagen) to give T7 expression vector pRSF-LF. The resulting plasmid was sequenced and shown to be free of mutations.

Expression and purification of LF protease. E. coli BL21(DE3) cells (1L) transformed with pRSF-LF plasmid were grown to mid-log phase ($OD_{600} \approx 0.5$) in LB medium containing

kanamycin (34 mg/L) and induced with 0.15 mM IPTG at 22°C for 16 hours. The cells were pelleted by centrifugation, resuspended in 30 mL of lysis buffer and lysed by sonication. The lysate was clarified by centrifugation and purified on Ni-NTA agarose beads as described above. The protein was eluted with column buffer containing 100 mM EDTA and dialyzed against LF reaction buffer (10 μM $CaCl_2$, 100 μM $ZnCl_2$, 10 mM $MgCl_2$, 20 mM NaPi, 100 NaCl buffer at pH 7.2). The purified protein was quantified by UV spectroscopy using an extinction coefficient per chain at 280 nm of 79,650 $M^{-1}cm^{-1}$, and characterized by SDS-PAGE and ES-MS (calculated molecular weight: 92949.0 Da, observed mass: 92980 ± 20 Da). The enzymatic activity of the LF protease was tested against the consensus peptide and the different FRET reporter constructs.

In vitro LF proteolytic assay using HPLC. An HPLC-based LF proteolytic assay was performed by incubating the consensus peptide (200 μM) with LF (10 μM) in 500 μL of LF reaction buffer at 37°C for 30 minutes and analyzed by HPLC and ES-MS.

In-vitro FRET-based LF proteolytic assay. The enzymatic assay was performed by incubating the different FRET reporter constructs (**1** to **5**, 10 nM) with purified LF protease (10 nM) in 3 mL of LF reaction buffer in a quartz cuvette. The reaction was kept with gentle stirring at 37°C for up to 180 minutes. Reaction progress was continuously monitored by fluorimetry using a Spex FluoroLog-3 spectrofluorometer with both excitation and emission slits set at 5 nm. For FRET measurements, the excitation wavelength was set to 414 nm and fluorescence scans were carried out at a rate of 2 nm/s from 450 nm to 600 nm. The relative FRET ratio change was calculated as previously reported [24] using: $FRC = [(I_t^{525} / I_t^{475}) / (I_0^{525} / I_0^{475})]$, where I_0 and I_t are the fluorescence intensities at time zero and at particular time (t), respectively, either at 525 nm or 475 nm.

*Sequential expression of FRET reporter **6** and LF protease. E. coli* BL21(DE3) cells were transformed sequentially with plasmid pBAD-6 and pRSF-LF. The resulting cells were grown at 37°C to mid-log phase ($OD_{600} \approx 0.5$) in LB media containing ampicillin (100 mg/L) and kanamycin (34 mg/L), and supplemented with 0.5 % glucose. Expression of FRET-based protein reporter **6** was induced by adding 1/100th culture volume of 20% w/v of L-arabinose for 8 hours at 30°C. During this period, an aliquot of L-arabinose was added every 4 hours. After the induction period, cells were incubated at 22°C overnight and then pelleted by centrifugation. The cells were washed once and then resuspended in minimal media M9 containing glycerol (4 mL/L) as the sole carbon source, then supplemented with ampicillin (100 mg/L) and kanamycin (34 mg/L). Prior to the induction with IPTG, a 10 mL sample of cells was taken for fluorescence analysis. The rest of the cells were induced with 0.25 mM IPTG at 30°C. Small aliquots of cells were taken at different time points for fluorescence analysis.

In vivo FRET-based analysis of LF protease activity. Cell aliquots (1 mL) were briefly centrifuged at 5,000 rpm for 30 seconds, washed three times with 1 mL of PBS (20 mM NaP_i, 100 mM NaCl buffer at pH 7.2), and resuspended in 1 mL of PBS. The concentration of cells was finally adjusted to an OD_{600} of 0.6 with PBS. Cell samples (100 µL) were mixed with 2.9 mL of PBS in a quartz cuvette kept at 37°C. The samples were gently stirred with a magnetic stir bar. Fluorescence analysis was performed as described in the *in vitro* experiments (see above). Protein concentrations were quantified by fluorescence using excitation and emission wavelengths of 490 nm and 525 nm, respectively, and then compared against the 525nm emission of purified FRET reporter of a known concentration previously calculated by UV-vis.

Results and Discussion

Molecular design, expression, and purification of FRET-based reporters for LF protease activity

The different LF FRET reporters (**1** to **5**) were constructed by fusing two optimized fluorescent proteins (CyPet and YPet) [24] to a consensus LF recognition sequence [36] (Figure 1). The CyPet–Ypet pair was originally obtained by evolutionary optimization from cyan fluorescent protein (CFP) and yellow fluorescent protein (YFP) by Daugherty and co-workers [24]. This optimized FRET pair enables intracellular FRET measurements with enhanced sensitivity and dynamic range, and thus allows the use of standard flow cytometry instrumentation for high-throughput analysis and screening applications [39]. This is critical for performing screening assays inside living cells. The LF consensus sequence was derived from a peptide obtained by Cantley and co-workers [36] from the analysis of partially degenerated peptide libraries to provide an optimal substrate for LF protease. This peptide incorporates consensus residues (P5-P4') surrounding the scissile bond based on the peptide library screen, flanked by residues from MAPKK2. The crystal structure of this peptide with an inactive form of LF showed that nine residues of the substrate (from P3 to P6') bind in an extended conformation along the 40 Å–long substrate recognition groove [36; 40]. Thus, in order to release any potential steric hindrance introduced by the two flanking fluorescent proteins on the peptide substrate, we designed several FRET-based reporters (**1** to **5**) encoding several repeats of the flexible tripeptide Gly-Gly-Ser [41] between the LF substrate and the CyPet and YPet fluorescent proteins (Figure 1).

Characterization of all the genetically encoded FRET-based reporters was carried out first *in vitro*. For this purpose, constructs **1** to **5** were first cloned onto a T7-driven bacterial

expression vector, expressed in *E coli* and readily purified using Ni-NTA affinity chromatography. All the FRET reporters showed high expression levels (≈ 10 mg of pure protein per liter of culture), and were characterized by ES-MS and SDS-PAGE (Figures 1 and 2).

Fluorescence properties of FRET-based reporters 1 to 5

Protein constructs **1** to **5** were analyzed by fluorescence spectroscopy to evaluate their FRET efficiency in the "on" state. In all the cases, CyPet–YPet fusion proteins showed high FRET values when excited at 414 nm. The FRET values, estimated as the ratio between the fluorescence intensities at 525 nm (maximum emission for YPet) and 475 nm (maximum emission for CyPet), ranged from 9.5 for construct **5** to 6.2 for construct **6** (see Figure 1). In contrast, an equimolar solution of YPet and CyPet gave a FRET value of only 0.7. As expected, increasing the length of the flexible linker $(Gly\text{-}Gly\text{-}Ser)_n$ decreased the FRET efficiency of the corresponding reporter proteins around 35% (construct **1** versus **6**). It is interesting to note, however, the relatively high FRET values observed for constructs **4** and **5**. These constructs contain 8 and 12 Gly-Gly-Ser repeats, which in a completely extended conformation have lengths of 78 Å and 116 Å, respectively. These values are well beyond the Foster radius (≈50 Å) assigned for the FRET pair formed by cyan and yellow fluorescent proteins [41]. Recent studies by Merkx and co-workers [41; 42] on the effect of flexible linkers in FRET-based biosensors have shown similar results, indicating that the behavior of these flexible linkers can be better described as random coils using either a worm-like chain or Gaussian chain model rather than as a totally extended conformation.

Expression and enzymatic activity of recombinant LF protease

The LF protease employed in this work was cloned from *B. anthracis* strain Sterne [20] into a T7-driven pRSF bacterial expression plasmid [43]. The protein was readily expressed in *E.*

coli and purified by Ni-NTA chromatography. A total of 10 mg of purified LF protease per liter of *E. coli* culture was routinely obtained. The activity of recombinantly expressed LF protease was tested using consensus peptide H-RRKKVYPYPMEGTIA-NH_2 as a substrate in a 200:1 peptide-to-enzyme ratio. The cleavage reaction was monitored by analytical RP-HPLC indicating that the protease was totally active. LF was able to cleave specifically the peptide bond between P1-P1' residues of the peptide substrate in less than 15 minutes (data not shown) using the conditions described under Materials and Methods.

***In vitro* cleavage of FRET-based reporters 1 to 5 by LF protease**

LF cleavage of FRET reporters **1** to **5** was monitored by fluorescence spectroscopy. This was carried out by treating a 10 nM solution of the corresponding FRET reporter with different amounts of purified LF protease at 37°C in LF reaction buffer. Under these conditions, all constructs showed between a 9- to 14-fold decrease in FRET signal upon cleavage with LF (Figure 3). Cleavage reactions were also monitored by SDS-PAGE (Figure 3B) confirming that the proteolytic cleavage was specifically taking place at the linker located between the two fluorescent proteins. As the cleavage reaction progressed, the initial band ≈57 kDa corresponding to the FRET reporter disappeared giving rise to a doublet of bands around 28 kDa. The FRET value once the cleavage was complete was estimated to be ≈ 0.7 in all the constructs. This value is similar to that found for an equimolar mixture of CyPet and YPet proteins.

We also explored the effect of the linker length on the efficiency of LF protease cleavage. As expected, the cleavage reaction proceeds more efficiently as the length of the flexible linker Gly-Gly-Ser increases. As shown if Figure 3C, the change in half-life time is more pronounced when we compare constructs **1** to **3**. In each case, cleavage occurs about twice as fast with each pair of Gly-Gly-Ser repeats added, with $\tau_{1/2}$ values of 33, 17, and 9 minutes, respectively.

Constructs **3** to **6**, however, showed very similar half-life times under the same reaction conditions, showing only a marginal increase in the rate of cleavage ($\tau_{1/2}$ values for constructs **3**, **4,** and **5** were 10, 9, and 8 minutes, respectively). These results confirm that the presence of two Gly-Gly-Ser repeats on each side of the LF recognition sequence is enough to release most of the steric hindrance introduced by the presence of the two large fluorescent proteins.

The cleavage of the FRET-based reporter by LF was also shown to be dose-dependent on the concentration of LF thus indicating that the cleavage was specific for the consensus sequence embedded in the FRET-based reporter protein. As shown in Figure 3D, the initial rate of cleavage for construct **3** was shown to be proportional to the concentration of LF used in a range from 10 to 100 nM. These results show the potential of these constructs to be used as a sensitive LF probe able to detect nM concentrations of LF protease *in vitro*.

Design of an LF protease FRET reporter system in live *E. coli* cells

Our next step was to explore the possibility of using a FRET-based reporter to work inside living *E. coli* cells for the *in vivo* screening of LF inhibitors. Key to this was the use of two orthogonal plasmids with tightly controlled inducible promoters for individual expression of LF protease and its FRET-based substrate (Figure 4). This was accomplished using the pRSF and pBAD families of expression vectors for the selective expression of LF and its FRET-based reporter, respectively.

Based on our previous results, we decided to use an intracellular reporter with six Gly-Gly-Ser repeats on each side of the LF recognition sequence. This long linker allows rapid cleavage of the LF recognition sequence while still showing a relatively high dynamic range for FRET change upon cleavage. This new construct (**6**, see Figure 1), which is virtually identical to **5**, was cloned into an expression pBAD-derived vector to give the plasmid pBAD-6. This

expression plasmid contains an araBAD-driven promoter and a p15 replicon. LF was cloned into a pRSF-based vector to give the expression plasmid pRSF-LF described earlier. This expression vector contains a T7-driven promoter and an RSF origin of replication [43]. These two expression plasmids are fully compatible for the sequential expression of proteins in *E. coli* cells, and they have been used for the study of protein–protein interactions *in vivo* [44].

In vivo sensing of LF activity

In order to explore the potential of construct **6** to optically sense LF activity inside living cells, plasmids pBAD-6 and pRSF-6 were co-transformed into *E. coli* BL21(DE3) cells. Induction of FRET reporter **6** was performed first by inducing the cells overnight with L-arabinose. Because the cells employed in this experiment were capable of metabolizing L-arabinose, two more aliquots of L-arabinose were added every 4 hours during the first 8 hours of induction. The cells were also supplemented with glucose to repress any residual expression of LF during this time. The presence of glucose is known to repress both araBAD and T7/lac promoters [45; 46], but in the presence of L-arabinose the reporter protein was expressed, albeit at a slower rate [44; 46]. At this point the cells were harvested and resuspended in minimal media M9. An aliquot of these cells was analyzed by fluorescence spectroscopy (Figure 5). The fluorescence spectrum revealed the presence of a strong FRET emission signal at 525 nm indicating the presence of reporter protein **6**. The *in vivo* FRET value (estimated as the ratio between the fluorescence intensities at 525 nm and 475 nm) for construct **6**, however, was smaller than the reported for construct **5** *in vitro* (3.4 versus 6.2). Intrigued by this difference, because reporters **5** and **6** share the same linker composition, we decided to express reporter **6** using the same conditions as before but employing *E. coli* cells transformed only with pBAD-6 instead. The fluorescence analysis of the resulting cells provided a similar FRET value thus

ruling out the presence of any prematurely expressed LF as the cause for the smaller FRET value observed for construct **6** *in vivo*. Based on these results, it is very likely that the observed decrease in FRET efficiency inside living cells could be due to a non-specific interaction between the reporter protein and some unidentified component of the cellular background.

Next, we decided to express LF and evaluate the ability of construct **6** to sense its activity *in vivo*. The previously induced fluorescent cells resuspended in M9 were complemented with glycerol and the appropriate antibiotic, and then induced with IPTG at 30°C. The proteolytic reaction was monitored by taking small aliquots of cells at different times and measuring their fluorescence spectra. Within 1 hour of induction, the FRET signal decreased from a value of 3.4 ("FRET-on" state) to 0.9 ("FRET-off" state) as shown in Figure 5. Longer induction times of up to 5 hours gave similar fluorescence spectra and FRET ratios, indicating the cleavage reaction was completed in less than 1 hour. Moreover, the FRET-off state observed *in vivo* was practically identical to the value observed *in vitro,* further confirming the total cleavage of the reporter protein *in vivo*.

Quantification of the YPet protein before and after LF induction indicated that the concentration of YPet remains constant and therefore no more reporter protein was expressed during the induction of LF (Figure 5B). Furthermore, the intracellular concentration of construct **6** was estimated to be ≈ 20 μM. At these concentration levels, the propensity of cleaved CyPet and YPet to heterodimerize, thus increasing the FRET signal, is minimal [24; 39]. These results confirm that the change in FRET signal was due only to proteolytic cleavage.

Our results show that *E. coli* cell strains co-transformed with pBAD-6 and pRSF-LF can be efficiently used for *in vivo* screening of libraries of compounds. Key to our approach is to maintain LF and its substrate under the control of two tightly regulated and inducible promoters.

This allows for discrimination between the FRET-on state, where only the substrate is expressed, and the FRET-off state, where LF is expressed in the presence on the substrate (Figure 5). Hence, addition or expression, by the same cell, of any potential LF inhibitor during the FRET-on state can be readily screened by measuring the FRET ratio at different times during the induction of LF. Potential inhibitors will inhibit the cleavage of the substrate at early times of LF induction. In contrast, cells containing non-inhibitors will efficiently cleave the substrate, rapidly reaching the FRET-off state.

Summary and conclusions

In summary, we have designed several genetically encoded FRET-based reporters specific for the anthrax LF protease. These reporters consist of an optimized FRET pair of fluorescent proteins, YPet and CyPet, which were recently described by Daugherty and co-workers [24] for the study of molecular interactions *in vivo* [39]. The CyPet and YPet proteins were linked together by a flexible linker containing a consensus recognition site for LF protease [36] flanked at both its N- and C-termini by several repeats of the flexible tripeptide Gly-Gly-Ser [41]. *In vitro* evaluation of the different reporters showed that at least a minimum of two Gly-Gly-Ser repeats are required at each side of the LF peptide recognition motif for efficient cleavage by LF. Interestingly, the introduction of multiple Gly-Gly-Ser repeats in the linker between the CyPet and YPet fluorescent proteins had a relatively minor effect on the FRET efficiency of the protein constructs containing the longer linkers. This interesting effect has also been recently reported by Merkx and coworkers [41; 42] and it has been explained by the extremely flexible nature of these linkers [41]. *In vitro* evaluation of the different FRET reporters showed between a 9- and 14-fold decrease in FRET signal upon cleavage with LF.

Optimized FRET reporter **5** was used next in the design of a cell-based FRET reporter for LF activity. This approach employs bacterial cells as individual micro-reactors where the substrate and the enzyme (i.e., LF protease) are sequentially expressed. This was accomplished by cloning FRET reporter **6** and LF into two compatible, tightly controlled and inducible expression plasmids. We have shown that *E. coli* cells co-transformed with both plasmids can be induced into either the FRET-on or FRET-off states by expressing only the reporter protein or both sequentially, respectively. The FRET signal of living bacteria induced to express reporter **6** decreased approximately 5 times in less than 1 hour upon induction of LF expression.

This result opens the possibility for *in vivo* screening of genetically encoded libraries against LF. Recent advances in the fields of protein engineering have allowed for the first time the biosynthesis of circular peptides inside living cells [31]. We have recently used two natural disulfide-containing cyclic peptides, the cyclotides Kalata B1 and MCoTI-II, and the Bowman-Birk sunflower trypsin inhibitor (SFTI-1) as templates for the *in vivo* biosynthesis of peptide libraries using protein splicing units [32; 47]. These types of scaffolds have a tremendous potential for the development of therapeutic leads based on their extraordinary stability and potential for grafting applications [48; 49]. We envision the combination of our cell-based fluorescent LF reporter with the generation of cyclic peptide-based libraries will provide a promising alternative approach for the high-throughput screening of large biological-based combinatorial libraries using FACS.

Acknowledgements

This work was performed under the auspices of the U.S. Department of Energy by the University of California, Lawrence Livermore National Laboratory under contract No. W-7405-Eng-48.

Figure Captions

Figure 1. Genetically encoded FRET reporters used in this work. Single letter codes are used to represent the LF recognition sequence and flexible linker. Expected masses were calculated for the mature proteins without N-terminal methionine.

Figure 2. Expression and purification of FRET reporter protein **2**. A. Gradient SDS-PAGE analysis of bacterial cell lysate expressing reporter **2** (line 1) and after purification by Ni-NTA affinity chromatography (line 2). B. ES-MS analysis of purified FRET reporter **2**.

Figure 3. *In vitro* cleavage of FRET reporter **1** to **5** by LF protease. A. Fluorescence spectra of a 10 nM solution of construct **3** incubated with LF (100 nM) at different time points. Excitation was done at 413 nm. B. Analysis of the proteolytic cleavage of construct **3** by gradient SDS-PAGE. C. Effect of the Gly-Gly-Ser linker length on the cleavage rate by LF. D. Fluorescence analysis of a 10 nM solution of construct **3** cleaved with different concentrations of LF protease. The FRET ratio change was calculated as described under Materials and Methods.

Figure 4. Scheme employed for the production of a cell-based reporter for screening LF activity inside living bacterial cells.

Figure 5. A. *In vivo* cleavage of FRET reporter **6** followed by fluorescence spectroscopy. A. Fluorescence spectra of *E. coli* cells expressing reporter **6** in the presence (green line) or absence (red line) of LF. B. Quantification of fluorescent protein YPet was performed on live *E. coli* cells expressing reporter **6** in the presence (green line) or absence (red line) of LF. Cells were excited at 490 nm.

Table 1. Oligonucleotides used to encode different LF recognition sites containing a variable number of $(Gly\text{-}Gly\text{-}Ser)_n$ repeats.

Construct **1** p5: 5'-GAT CCC GTC GTA AAA AAG TTT ATC CGT ATC CGA TGG AAG GTA CCA TCG CCC A-3' p3: 5'-AGC TTG GGC GAT GGT ACC TTC CAT CGG ATA CGG ATA AAC TTT TTT ACG ACG G-3'
Construct **2** p5: 5'-GAT CCG GTG GCA GCC GTC GTA AAA AAG TTT ATC CGT ATC CGA TGG AAC CGA CCA TCG CCG GTG GCA GCC A-3' p3: 5'-AGC TTG GCT GCC ACC GGC GAT GGT CGG TTC CAT CGG ATA CGG ATA AAC TTT TTT ACG ACG GCT GCC ACC G-3'
Construct: **3** p5: 5'- GAT CCG GTG GCA GCG GTG GCA GCC GTC GTA AAA AAG TTT ATC CGT ATC CGA TGG AAC CGA CCA TCG CCG GTG GCA GCG GTG GCA GCC A-3' p3: 5'- AGC TTG GCT GCC ACC GCT GCC ACC GGC GAT GGT CGG TTC CAT CGG ATA CGG ATA AAC TTT TTT ACG ACG GCT GCC ACC GCT GCC ACC G-3'
Construct: **4** p5a: 5'-GAT CCG GTG GCA GCG GTG GCA GCG GTG GCA GCG GTG GCA GCC GTC GTA AAA AAG TTT ATC C-3' p3a: : 5'-GAT ACG GAT AAA CTT TTT TAC GAC GGC TGC CAC CGC TGC CAC CGC TGC CAC CGC TGC CAC CG-3' p5b: 5'- GTA TCC GAT GGA ACC GAC CAT CGC CGG TGG CAG CGG TGG CAG CGG TGG CAG CGG TGG CAG CCA-3' p3b: 5'- AGC TTG GCT GCC ACC GCT GCC ACC GCT GCC ACC GCT GCC ACC GGC GAT GGT CGG TTC CAT CG-3'
Construct: **5** p5a: 5'- GAT CCG GTG GCA GCG GTG GCA GCG GTG GCA GCG GTG GCA GCG GTG GCA GCG GTG GCA GCC GTC GTA AAA AAG TTT ATC C-3' p3a: 5'- GAT ACG GAT AAA CTT TTT TAC GAC GGC TGC CAC CGC TGC CAC CGC TGC CAC CGC TGC CAC CGC TGC CAC CGC TGC CAC CG-3' p5b: 5'- GTA TCC GAT GGA ACC GAC CAT CGC CGG TGG CAG CGG TGG CAG CGG TGG CAG CGG TGG CAG CGG TGG CAG CCA-3' p3b: 5'- AGC TTG GCT GCC ACC GCT GCC ACC GCT GCC ACC GCT GCC ACC GCT GCC ACC GCT GCC ACC GCT GCC ACC GGC GAT GGT CGG TTC CAT CG-3'

References

[1]S.H. Leppla, Anthrax toxin edema factor: a bacterial adenylate cyclase that increases cyclic AMP concentrations of eukaryotic cells. Proc. Natl. Acad. Sci. U S A 79 (1982) 3162-3166.

[2]K.R. Klimpel, N. Arora, and S.H. Leppla, Anthrax toxin lethal factor contains a zinc metalloprotease consensus sequence which is required for lethal toxin activity. Mol. Microbiol. 13 (1994) 1093-1100.

[3]C. Montecucco, F. Tonello, and G. Zanotti, Stop the killer: how to inhibit the anthrax lethal factor metalloprotease. Trends Biochem. Sci. 29 (2004) 282-285.

[4]K.A. Bradley, J. Mogridge, M. Mourez, R.J. Collier, and J.A. Young, Identification of the cellular receptor for anthrax toxin. Nature 414 (2001) 225-229.

[5]H.M. Scobie, G.J. Rainey, K.A. Bradley, and J.A. Young, Human capillary morphogenesis protein 2 functions as an anthrax toxin receptor. Proc. Natl. Acad. Sci. U S A 100 (2003) 5170-5174.

[6]E. Santelli, L.A. Bankston, S.H. Leppla, and R.C. Liddington, Crystal structure of a complex between anthrax toxin and its host cell receptor. Nature 430 (2004) 905-908.

[7]V.M. Gordon, K.R. Klimpel, N. Arora, M.A. Henderson, and S.H. Leppla, Proteolytic activation of bacterial toxins by eukaryotic cells is performed by furin and by additional cellular proteases. Infect. Immun. 63 (1995) 82-87.

[8]J.C. Milne, D. Furlong, P.C. Hanna, J.S. Wall, and R.J. Collier, Anthrax protective antigen forms oligomers during intoxication of mammalian cells. J. Biol. Chem. 269 (1994) 20607-20612.

[9]J.M. Park, F.R. Greten, Z.W. Li, and M. Karin, Macrophage apoptosis by anthrax lethal factor through p38 MAP kinase inhibition. Science 297 (2002) 2048-2051.

[10]J.E. Kirby, Anthrax lethal toxin induces human endothelial cell apoptosis. Infect. Immun. 72 (2004) 430-439.

[11]A. Agrawal, J. Lingappa, S.H. Leppla, S. Agrawal, A. Jabbar, C. Quinn, and B. Pulendran, Impairment of dendritic cells and adaptive immunity by anthrax lethal toxin. Nature 424 (2003) 329-334.

[12]M. Forino, S. Johnson, T.Y. Wong, D.V. Rozanov, A.Y. Savinov, W. Li, R. Fattorusso, B. Becattini, A.J. Orry, D. Jung, R.A. Abagyan, J.W. Smith, K. Alibek, R.C. Liddington, A.Y. Strongin, and M. Pellecchia, Efficient synthetic inhibitors of anthrax lethal factor. Proc. Natl. Acad. Sci. U S A 102 (2005) 9499-9504.

[13]Y. Xiong, J. Wiltsie, A. Woods, J. Guo, J.V. Pivnichny, W. Tang, A. Bansal, R.T. Cummings, B.R. Cunningham, A.M. Friedlander, C.M. Douglas, S.P. Salowe, D.M. Zaller, E.M. Scolnick, D.M. Schmatz, K. Bartizal, J.D. Hermes, M. MacCoss, and K.T. Chapman, The discovery of a potent and selective lethal factor inhibitor for adjunct therapy of anthrax infection. Bioorg. Med. Chem. Let.t 16 (2006) 964-968.

[14]L.M. Mullen, S.P. Nair, J.M. Ward, A.N. Rycroft, and B. Henderson, Phage display in the study of infectious diseases. Trends Microbiol. 14 (2006) 141-147.

[15]S.E. Hammond, and P.C. Hanna, Lethal factor active-site mutations affect catalytic activity in vitro. Infect. Immun. 66 (1998) 2374-2378.

[16]N.S. Duesbery, C.P. Webb, S.H. Leppla, V.M. Gordon, K.R. Klimpel, T.D. Copeland, N.G. Ahn, M.K. Oskarsson, K. Fukasawa, K.D. Paull, and G.F. Vande Woude, Proteolytic inactivation of MAP-kinase-kinase by anthrax lethal factor. Science 280 (1998) 734-737.

[17]G. Vitale, L. Bernardi, G. Napolitani, M. Mock, and C. Montecucco, Susceptibility of mitogen-activated protein kinase kinase family members to proteolysis by anthrax lethal factor. Biochem. J. 352 (2000) 739-745.
[18]M. Mock, and B.P. Roques, Progress in rapid screening of Bacillus anthracis lethal factor activity. Proc. Natl. Acad. Sci. U S A 99 (2002) 6527-6529.
[19]F. Tonello, M. Seveso, O. Marin, M. Mock, and C. Montecucco, Screening inhibitors of anthrax lethal factor. Nature 418 (2002) 386.
[20]Y. Kwon, K. Welsh, A.R. Mitchell, and J.A. Camarero, Preparation of peptide p-nitroanilides using an aryl hydrazine resin. Org. Lett. 6 (2004) 3801-3804.
[21]I.A. Schepetkin, A.I. Khlebnikov, L.N. Kirpotina, and M.T. Quinn, Novel small-molecule inhibitors of anthrax lethal factor identified by high-throughput screening. J. Med. Chem. 49 (2006) 5232-5244.
[22]N.C. Shaner, P.A. Steinbach, and R.Y. Tsien, A guide to choosing fluorescent proteins. Nat. Methods 2 (2005) 905-909.
[23]B.N. Giepmans, S.R. Adams, M.H. Ellisman, and R.Y. Tsien, The fluorescent toolbox for assessing protein location and function. Science 312 (2006) 217-224.
[24]A.W. Nguyen, and P.S. Daugherty, Evolutionary optimization of fluorescent proteins for intracellular FRET. Nat. Biotechnol. 23 (2005) 355-360.
[25]K.T. Boulware, and P.S. Daugherty, Protease specificity determination by using cellular libraries of peptide substrates (CLiPS). Proc. Natl. Acad. Sci. USA 103 (2006) 7583-7588.
[26]I. Kaganman, FRETting for a more detailed interactome. Nat. Methods 4 (2007) 112-113.
[27]J.A. Camarero, and T.W. Muir, Biosynthesis of a Head-to-Tail Cyclized Protein with Improved Biological Activity. J. Am. Chem. Soc. 121 (1999) 5597-5598.
[28]C.P. Scott, E. Abel-Santos, M. Wall, D. Wahnon, and S.J. Benkovic, Production of cyclic peptides and proteins in vivo. Proc. Natl. Acad. Sci. USA 96 (1999) 13638-13643.
[29]J.W. Trauger, R.M. Kohli, H.D. Mootz, M.A. Marahiel, and C.T. Walsh, Peptide cyclization catalysed by the thioesterase domain of tyrocidine synthetase. Nature 407 (2000) 215-218.
[30]R.M. Kohli, C.T. Walsh, and M.D. Burkart, Biomimetic synthesis and optimization of cyclic peptide antibiotics. Nature 418 (2002) 658-661.
[31]R. Kimura, and J.A. Camarero, Expressed protein ligation: a new tool for the biosynthesis of cyclic polypeptides. Protein Pept. Lett. 12 (2005) 789-794.
[32]R.H. Kimura, A.T. Tran, and J.A. Camarero, Biosynthesis of the cyclotide kalata B1 by using protein splicing. Angew. Chem. Int. Ed. Engl. 45 (2006) 973-976.
[33]W. Wang, C. Mulakala, S.C. Ward, G. Jung, H. Luong, D. Pham, A.J. Waring, Y. Kaznessis, W. Lu, K.A. Bradley, and R.I. Lehrer, Retrocyclins kill bacilli and germinating spores of Bacillus anthracis and inactivate anthrax lethal toxin. J. Biol. Chem. 281 (2006) 32755-32764.
[34]C. Kim, N. Gajendran, H.W. Mittrucker, M. Weiwad, Y.H. Song, R. Hurwitz, M. Wilmanns, G. Fischer, and S.H. Kaufmann, Human alpha-defensins neutralize anthrax lethal toxin and protect against its fatal consequences. Proc. Natl. Acad. Sci. USA 102 (2005) 4830-4835.
[35]L.V. Lee, K.E. Bower, F.S. Liang, J. Shi, D. Wu, S.J. Sucheck, P.K. Vogt, and C.H. Wong, Inhibition of the proteolytic activity of anthrax lethal factor by aminoglycosides. J. Am. Chem. Soc. 126 (2004) 4774-4775.

[36]B.E. Turk, T.Y. Wong, R. Schwarzenbacher, E.T. Jarrell, S.H. Leppla, R.J. Collier, R.C. Liddington, and L.C. Cantley, The structural basis for substrate and inhibitor selectivity of the anthrax lethal factor. Nat. Struct. Mol. Biol. 11 (2004) 60-66.
[37]G.B. Fields, and R.L. Noble, Solid phase peptide synthesis utilizing 9-fluorenylmethoxycarbonyl amino acids. Int. J. Peptide Protein Res. 35 (1990) 161-214.
[38]V.K. Sarin, S.B.H. Kent, J.P. Tam, and R.B. Merrifield, Qunatitative monitoring of solid-phase peptide synthesis by the ninhydrin reaction. Anal. Biochem. 117 (1981) 147-157.
[39]X. You, A.W. Nguyen, A. Jabaiah, M.A. Sheff, K.S. Thorn, and P.S. Daugherty, Intracellular protein interaction mapping with FRET hybrids. Proc. Natl. Acad. Sci. USA 103 (2006) 18458-63.
[40]A.D. Pannifer, T.Y. Wong, R. Schwarzenbacher, M. Renatus, C. Petosa, J. Bienkowska, D.B. Lacy, R.J. Collier, S. Park, S.H. Leppla, P. Hanna, and R.C. Liddington, Crystal structure of the anthrax lethal factor. Nature 414 (2001) 229-233.
[41]T.H. Evers, E.M. van Dongen, A.C. Faesen, E.W. Meijer, and M. Merkx, Quantitative understanding of the energy transfer between fluorescent proteins connected via flexible peptide linkers. Biochemistry 45 (2006) 13183-13192.
[42]E.M. Dongen, T.H. Evers, L.M. Dekkers, E.W. Meijer, L.W. Klomp, and M. Merkx, Variation of Linker Length in Ratiometric Fluorescent Sensor Proteins Allows Rational Tuning of Zn(II) Affinity in the Picomolar to Femtomolar Range. J. Am. Chem. Soc. (2007) in press.
[43]T. Som, and J. Tomizawa, Origin of replication of Escherichia coli plasmid RSF 1030. Mol. Gen. Genet. 187 (1982) 375-383.
[44]D.S. Burz, K. Dutta, D. Cowburn, and A. Shekhtman, Mapping structural interactions using in-cell NMR spectroscopy (STINT-NMR). Nat. Methods 3 (2006) 91-93.
[45]T.H. Grossman, E.S. Kawasaki, S.R. Punreddy, and M.S. Osburne, Spontaneous cAMP-dependent derepression of gene expression in stationary phase plays a role in recombinant expression instability. Gene 209 (1998) 95-103.
[46]W.P. Boomershine, M.L. Raj, V. Gopalan, and M.P. Foster, Preparation of uniformly labeled NMR samples in Escherichia coli under the tight control of the araBAD promoter: expression of an archaeal homolog of the RNase P Rpp29 protein. Protein Expr. Purif. 28 (2003) 246-251.
[47]J.A. Camarero, R. Kimura, and A.T. Tran, A Cell-based Approach for Biosynthesis/Screening of Cyclic Peptide Libraries against Bacterial Toxins. J. Pept. Sci. 12 (2006) 89.
[48]D.J. Craik, S. Simonsen, and N.L. Daly, The cyclotides: novel macrocyclic peptides as scaffolds in drug design. Curr. Opin. Drug Discov. Devel. 5 (2002) 251-260.
[49]M.L. Korsinczky, H.J. Schirra, and D.J. Craik, Sunflower trypsin inhibitor-1. Curr. Protein Pept. Sci. 5 (2004) 351-364.

Figures

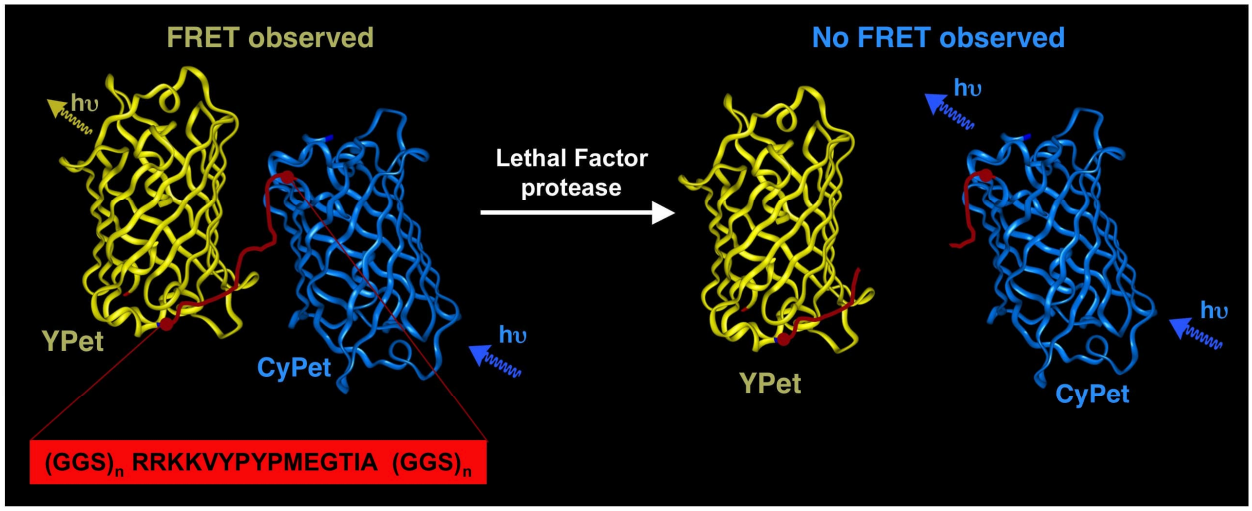

Construct	$(GGS)_n$	Vector	FRET-on ratio	Molecular Weight (Da)	
				Observed	Expected
1	0	pET28a-1	9.6	58110 ± 25	58072.7
2	1	pET28a-2	8.6	58516 ± 18	58515.1
3	2	pET28a-3	8.5	58922 ± 25	58917.5
4	4	pET28a-4	6.6	59721 ± 27	59722.2
5	6	pET28a-5	6.2	60547 ± 25	60526.9
6	6	pBAD-6	3.5	62353 ± 21	62353.9

Figure 1

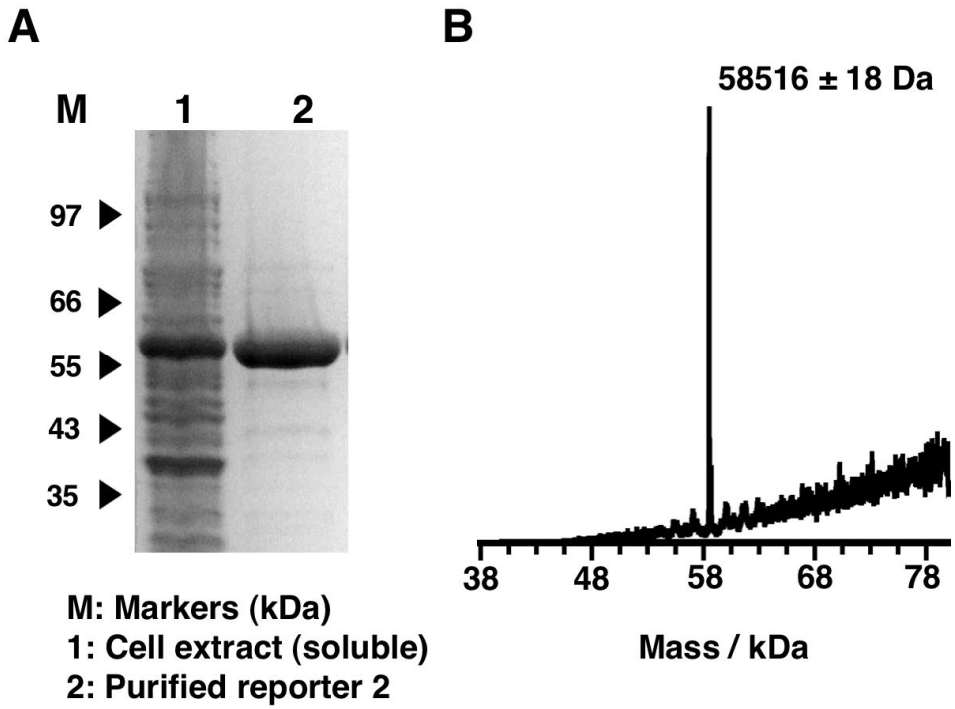
A
M
1
2
97
66
55
43
35
M: Markers (kDa)
1: Cell extract (soluble)
2: Purified reporter 2
B
58516 ± 18 Da
38
48
58
68
78
Mass / kDa

Figure 2

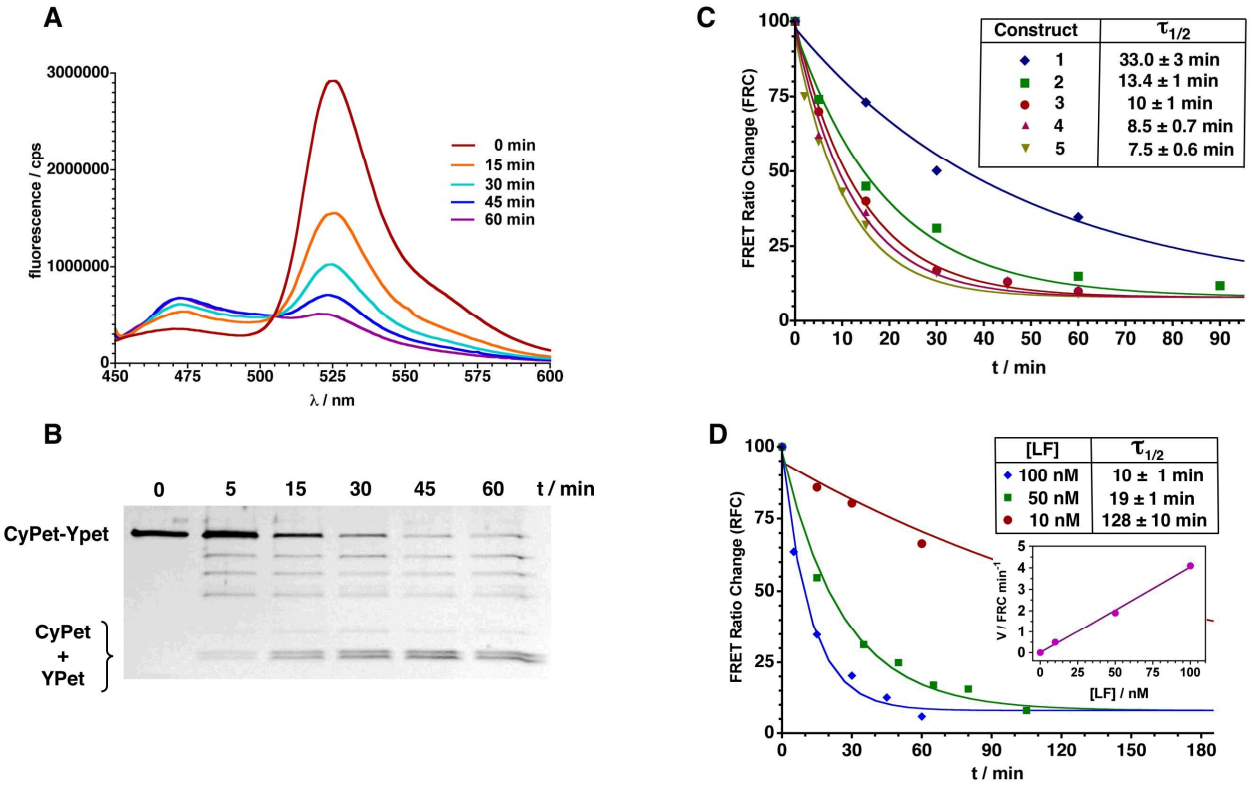
A
fluorescence / cps
3000000
2000000
1000000
0
450
475
500
525
550
575
600
λ / nm
0 min
15 min
30 min
45 min
60 min
B
0
5
15
30
45
60
t / min
CyPet-Ypet
CyPet
+
YPet
C
FRET Ratio Change (FRC)
100
75
50
25
0
0
10
20
30
40
50
60
70
80
90
t / min
Construct
τ1/2
1
33.0 ± 3 min
2
13.4 ± 1 min
3
10 ± 1 min
4
8.5 ± 0.7 min
5
7.5 ± 0.6 min
D
FRET Ratio Change (RFC)
100
75
50
25
0
0
30
60
90
120
150
180
t / min
[LF]
τ1/2
100 nM
10 ± 1 min
50 nM
19 ± 1 min
10 nM
128 ± 10 min
V / FRC min-1
5
4
3
2
1
0
0
25
50
75
100
[LF] / nM

Figure 3

Protein	Vector	Replicon	Resistance	Inducer	DNA
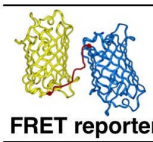 FRET reporter	pBAD-6	p15	Amp	Arabinose	
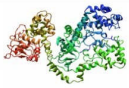 Anthrax LF	pRSF-LF	RSF102	Kan	IPTG	

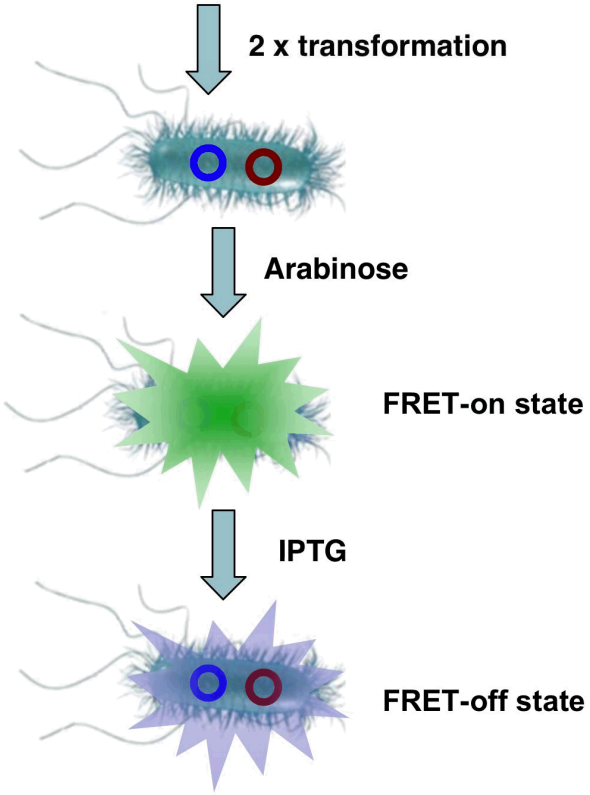

Figure 4

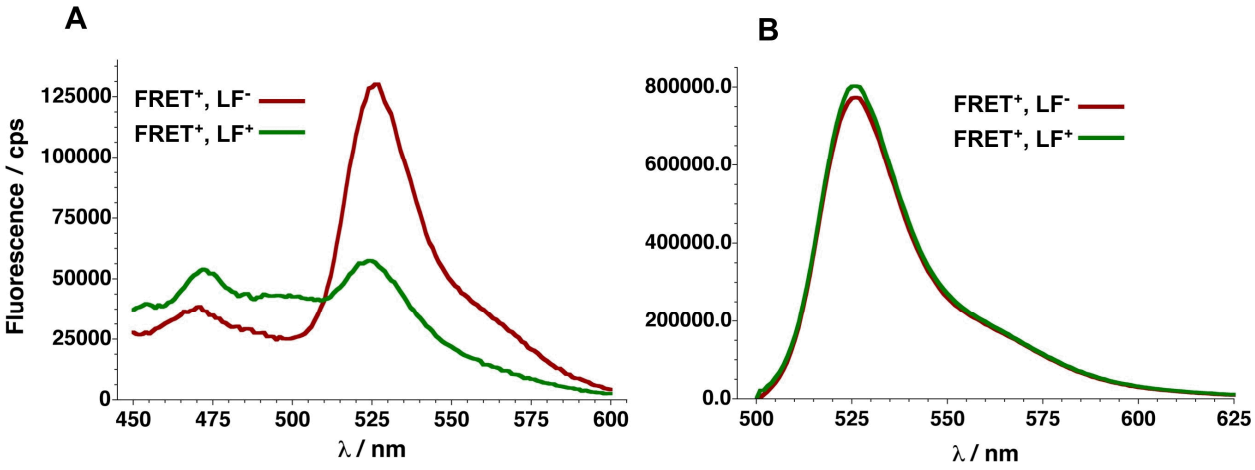
A
B
Fluorescence / cps
125000
100000
75000
50000
25000
0
450
475
500
525
550
575
600
λ / nm
FRET+, LF-
FRET+, LF+
800000.0
600000.0
400000.0
200000.0
0.0
500
525
550
575
600
625
λ / nm
FRET+, LF-
FRET+, LF+

Figure 5